Indian Journal of Biochemistry & Biophysics
Vol. 63, February 2026, pp. 127-136
DOI: 10.56042/ijbb.v63i2.22385

Hepatocyte lipoapoptosis as a mechanism of chronic liver injury in obese mice model: a close link with fetuin-A

Guria S, and Mukherjee S*

Endocrinology & Metabolism Laboratory, Department of Zoology, Siksha Bhavana (Institute of Science), Visva-Bharati (A Central University), Santiniketan-731 235, West Bengal, India

Received 04 August 2025; *revised 17 September 2025*

Obesity is a major risk factor for type 2 diabetes, cardiovascular diseases, hypertension, dyslipidemia, non-alcoholic fatty liver disease and several cancers. Liver, a vital metabolic organ and a primary insulin target, is vulnerable to high dietary fat. In conditions of obesity, the hepatic secretory profile of hepatokines is altered. One of the major hepatokines, fetuin-A (FetA) is over-secreted in obesity-induced diabetes and promotes insulin resistance and inflammation. The present study was undertaken to examine hepatocyte lipoapoptosis in obesity and the potential involvement of fetuin-A in such lipotoxicity. We used obese diabetic mice models by feeding high fat diet for different durations, short-term D1 (4-week), moderate-term D2 (16-week) and prolonged-term D3 (32-week). For understanding FetA effect, *in vivo* and *in vitro* experiments were carried out. Blood parameters, whole-body glucose tolerance, hepatocyte lipid and ROS accumulation, TUNEL assay, and immunoblotting analyses were performed. ROS induced apoptosis progressively in lipid-laden hepatocytes of obese diabetic mice. In FetA-treated mice, hepatic oxidative stress and histopathological alterations were observed. Hepatocyte apoptotic markers were elevated by FetA *in vivo* and *in vitro*. Taken together, the data implied pivotal role of FetA in mediating hepatocyte lipoapoptosis and thereby, exacerbating liver damage associated with obesity and type 2 diabetes.

Keywords: High fat diet, Insulin resistance, Liver, Obesity, Palmitate

The growing prevalence of obesity-induced diabetes in the current times is alarming. Excess calorie consumption and less-active sedentary living pattern are considered key drivers of this global pandemic. A hallmark pathophysiologic feature herein is 'insulin resistance', the loss of insulin sensitivity in the insulin target organs. The fact that obesity poses serious risks for developing type 2 diabetes, cardiovascular diseases, hypertension, dyslipidemia, non-alcoholic fatty liver disease and several cancer types[1] reinforces a strong correlation between obesity and metabolic complications. A gross imbalance of energy intake and energy expenditure culminates into obesity. At its centre stage is the adipose tissue, the main fat-storing tissue in the body. Excessive fat accumulation causes adipocyte hypertrophy, impaired adipocyte differentiation, altered secretory profile and enhanced lipolysis with adverse consequences of ectopic lipid deposition in the peripheral tissues, viz. skeletal muscle and liver[2]. In normal condition, insulin suppresses glycogenolysis in the liver and induces hepatic glycogen synthesis, thereby reducing overall glucose flux into the circulation. This process is hampered during insulin resistance[3]. Hepatic insulin insensitivity enhances *de novo* lipogenesis by activating transcription factors, SREBP1c and ChREBP, which promote hepatic lipid biosynthesis and accelerate progression of non-alcoholic fatty liver disease[4].

Apoptosis is a key factor in obesity-driven insulin resistance. Activation of JNK and subsequent caspase-2 and caspase-3 triggered apoptotic event in liver implying a close connection between insulin resistance and fatty liver progression[5]. A population-based study showed positive correlation between severity of insulin resistance and serum level of caspase 3-cleaved cytokeratin 18 (CK-18) fragments[6]. Activated caspases or CK-18 fragments combined with other methods are potential non-invasive means for detection of liver fibrosis[7,8]. Saturated fatty acid (SFA) overload can induce lipotoxicity and

*Correspondence:
E-mail: sutapa.mukherjee@visva-bharati.ac.in

Abbreviations: Apaf-1: Apoptotic Protease Activating Factor 1; ATM: Adipose Tissue Macrophage; BAX: Bcl-2-associated X protein; Bcl-2: B-cell lymphoma 2; CVD: Cardiovascular Disease; Cyt c: Cytochrome c; FetA: Fetuin-A; HFD: High Fat Diet; NAFLD: Non-Alcoholic Fatty Liver Disease; SD: Standard Diet; SFAs: Saturated Fatty Acids

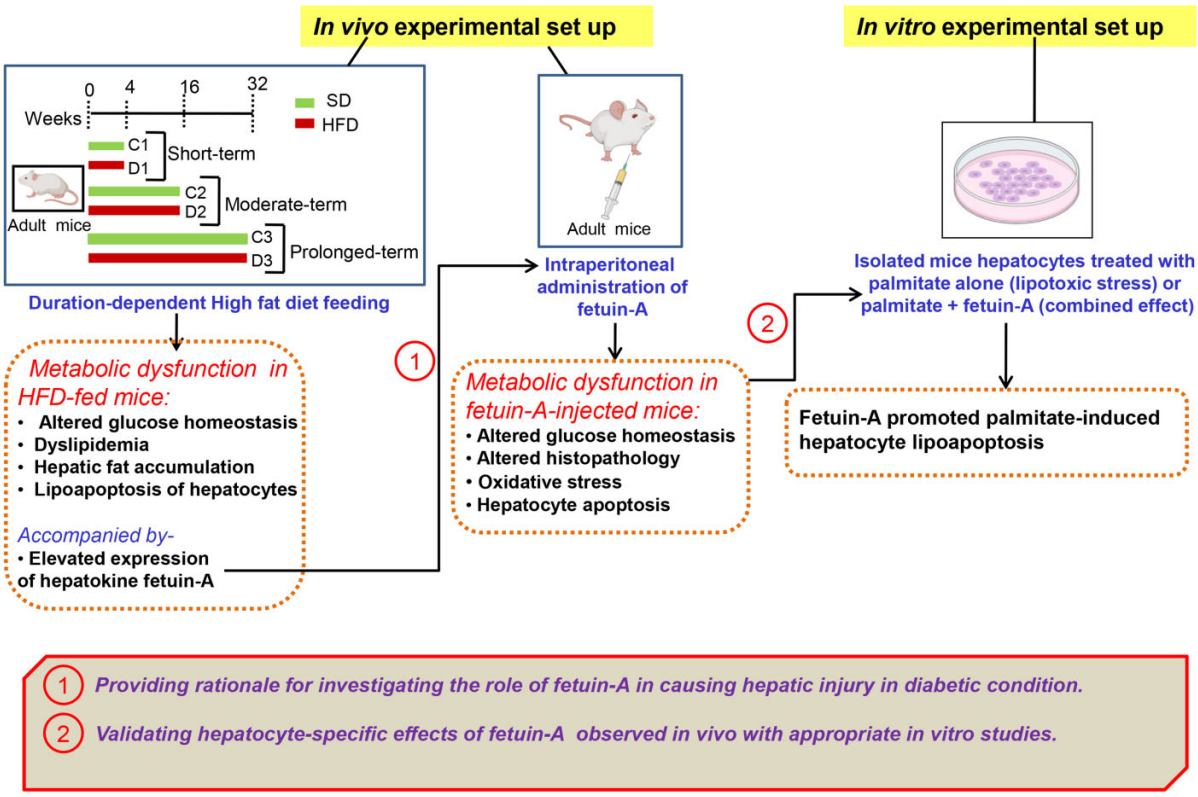

Graphical abstract

lipoapoptosis resulting in serious liver injury[9]. SFA can induce lipoapoptosis in hepatocytes through multiple intracellular responses involving activation of JNK, BAX and TLR4[10].

A wide range of molecules secreted from the liver named hepatokines are known to regulate glucose homeostasis, fat metabolism, and inflammation. However, in obese condition, hepatokine secretory pattern is altered which significantly contributes to metabolic diseases and associated complications[11]. Several evidences in animal models of diet-induced obesity as well as obese insulin-resistant subjects confirmed high circulating levels of fetuin-A (FetA), and have suggested FetA as a potential link between insulin resistance and fatty liver progression[12-14]. However, whether there is any involvement of FetA in triggering apoptosis in liver cells during obesity is not clearly known. In order to understand this particular aspect, we designed the present experiments using mice models of obesity-induced diabetes, and tested the effect of FetA both *in vivo* as well as *in vitro*. The findings highlight a crucial role of FetA vis-à-vis hepatocyte lipoapoptosis leading to liver damage associated with obesity and type 2 diabetes.

Materials and Methods

Chemicals and reagents

During the treatment, blood glucose monitoring was done using ACCU-CHEK glucometer (Roche Diagnostics GmbH, Germany). After sacrifice, blood glucose was quantified using a commercial kit (Reckon Diagnostic Pvt. Ltd., Vadodara, India). Lipid profile was measured using AUTOSPAN® Liquid GOLD Triglyceride test kit (ARKRAY Healthcare Pvt. Ltd., India). Oil Red O staining was done using Adipogenesis assay kit (Cayman Chemical, U.S.A). Fetuin-A ELISA kit was purchased from BT Lab, Shanghai, China. DeadEnd™ Fluorometric TUNEL (TdT-mediated dUTP Nick-End Labelling) assay kit was procured from Promega Corporation, Madison, U.S.A. All antibodies for immunoblotting were purchased from Santa Cruz Biotechnology, Inc, Dallas, Texas, U.S.A. Additional compounds were obtained from standard commercial sources and it was ensured that chemicals and reagents used were of analytical grade only.

Animal models

Animal handling, treatments and experiments were carefully conducted following the guidelines of the

Institutional Animal Ethics Committee (IAEC), Visva-Bharati (Permit No. 1819/GO/Re/S/15/CCSEA) under the aegis of the Committee for the Control and Supervision of Experiments on Animals (CCSEA), Govt. of India. Adult mice (8-week old, 20-22 g, Swiss albino male) were procured and reared in an ideal ambience of 25±2°C temperature, 55±5% relative humidity and 12:12 h light:dark cycle. The *in vivo* experimental sets of animals as used in the present study are shown (Fig. 1a). After initial acclimatization, mice were randomly divided into six groups (n=6 per group). Three sets of obese diabetic mice models were developed following three different durations of feeding with diet rich in saturated fat (~32% lard), namely, 4-week (short-term), 16-week (moderate-term) and 32-week (prolonged-term). In the increasing order of duration of treatment, high fat diet (HFD)-fed obese diabetic mice were denoted as D1, D2 and D3, respectively. The corresponding control mice groups (C1, C2 and C3) were fed with low-fat (~4.5%) containing standard diet (SD) following our earlier reports[15,16]. Another separate experimental set was raised with two groups of mice (n=6 per group): Control mice (C) and FetA-treated mice (F). For administration of FetA, mice were injected with FetA dissolved in phosphate buffered saline (PBS), pH 7.4 at 0.7 mg/g body weight for five consecutive days and then sacrificed for further experiments following our published protocol[16,17].

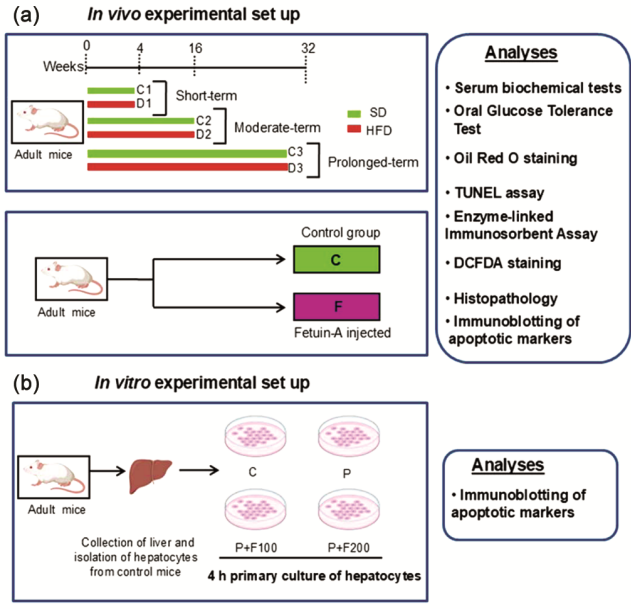

Fig. 1 — Schematic representation of (a) *in vivo*; and (b) *in vitro* experimental set ups and the various analyses carried out in the present study

Hepatocyte isolation, culture and treatments

After sacrifice, mice liver was perfused with PBS (pH 7.4) using a winged infusion set and collected in 0.9% (w/v) sterile normal saline. Hank's Balanced Salt Solution (HBSS) containing 5.5 mM glucose was used to clean the tissue. Liver was finely minced and digested in HBSS supplemented with 5% fatty acid-free bovine serum albumin (BSA), 5.5 mM glucose, and 3.2 mg/mL type II collagenase for 1 h in a water bath at 37ºC. The digested tissue was filtered through a fine mesh, and centrifuged at 2000 rpm for 10 min. The cell pellet was resuspended in fetal bovine serum-free culture media for further experiments. The cell suspension was introduced in each well of the six-well plate, containing 2 mL of FBS-free cell culture medium in CO_2 incubator at 37ºC for 1 h. Hepatocytes were treated without (control) and with palmitate only (0.75 mM), or palmitate conjugated-FetA at two different concentrations (100 µg/mL and 200 µg/mL) for 4 h *in vitro* as shown (Fig. 1b) following our previous work[16]. The cells were then lysed and subjected to immunoblotting analyses.

Body weight, blood glucose and serum parameters

Changes in body weight and blood glucose were regularly monitored throughout the treatment regimen. After sacrifice, glucose oxidase-peroxidase (GOD/POD) kit was used to estimate glucose level. Serum triglyceride levels were measured with a commercial kit following prescribed guidelines of the manufacturer.

Oral Glucose Tolerance Test (OGTT)

The oral glucose tolerance test was done by gavage of glucose solution (1 g/kg body weight). Blood glucose levels were recorded using ACCU-CHEK glucometer in blood samples drawn from tail vein of mice at 30 min intervals and continued up to 150 minutes. This test helped to assess the level of whole-body insulin sensitivity in mice from the ability of glucose clearance from the blood during glucose overload.

Enzyme-Linked Immunosorbent Assay (ELISA)

The levels of FetA were determined in sera obtained from control and treated mice using commercially available specific ELISA kit following the guidelines of the manufacturer.

Oil Red O staining

The isolated hepatocytes were fixed with 4% paraformaldehyde and stained with Oil Red O (ORO)

following manufacturer's protocol provided with the commercial kit. When ORO reaches fat droplets within hepatocytes, it leaves solvent and forms complex with lipid due to higher affinity. The fluorescent images of ORO-conjugated neutral fat inside liver cells were captured with confocal microscope (TCS-SP8, Leica Microsystems GmbH, Wetzlar, Germany). The counter staining of nuclei was done with DAPI, and fluorescence intensity was quantified using ImageJ (NIH) software.

DCFDA staining

The isolated hepatocytes were incubated with 10 µM probe 2',7'-dichlorodihydrofluorescein diacetate (H2-DCFDA) (Sigma-Aldrich, St. Louis, MO, USA) in a humidified incubator at 37 °C for 30 min. After washing cells with PBS pH 7.4, lysates were prepared. The subsequent measurements in a spectrofluorimeter (PerkinElmer, Inc., Waltham, MA) at excitation 488 nm and emission 522 nm quantified the fluorescence intensity of the oxidized product, 2',7'-dichlorodihydrofluorescein (DCF) in the samples.

TUNEL assay

The isolated hepatocytes were fixed in 4% paraformaldehyde and TUNEL assay was carried out with assay kit following manufacturer's instructions. DAPI was used as a counter stain. The labelled 3´-OH ends of fragmented DNA fluoresced bright green colour, and images were captured using confocal microscope (TCS-SP8, Leica Microsystems GmbH, Wetzlar, Germany). The percentage of TUNEL-positive cells in control and treated groups were recorded.

Histopathology

Liver tissues were placed in Bouin's fixative and passed through series of graded alcohols for proper dehydration. Tissue pieces were paraffinized and sectioned at 5 µm using a microtome. Hematoxylin and Eosin staining was carried out to observe tissue architecture and its alterations with upright bright-field microscope (DM3000 LED, Leica Microsystems GmbH, Wetzlar, Germany) at 200x and 400x magnifications.

Estimation of protein content

The isolated hepatocytes were lysed with RIPA lysis buffer (Sigma-Aldrich, St. Louis, MO, U.S.A.) and protease inhibitor cocktail (Sigma-Aldrich, St. Louis, MO, U.S.A.), and then sonicated. The ruptured cells were centrifuged at 12,000 rpm for 15 min at 4ºC, supernatant was collected as cell lysate and protein content was estimated[18] with bovine serum albumin as the standard.

Immunoblotting analyses

Equal amount of proteins was resolved in SDS-PAGE and transferred onto PVDF membrane (Millipore) by using Trans-Blot® apparatus (Bio-Rad laboratories). The membrane was blocked and incubated with respective primary antibodies overnight and then with alkaline phosphatase-tagged secondary antibody for 4 h. The protein bands were detected by substrate mix of BCIP (5-Bromo-4-chloroindole-3-yl phosphate)/NBT (nitro blue tetrazolium). The densitometric analyses were performed using ImageJ (NIH) software.

Statistical analyses

Data are presented as mean ± standard error of mean (SEM). Student's *t*-test, one-way ANOVA, two-way ANOVA followed by Tukey's post hoc test were used for comparisons between groups with GraphPad software. $P < 0.05$ was considered as minimal statistical significance.

Results and Discussion

Time-dependent effects of HFD upon body weight, glucose homeostasis, serum triglycerides, and hepatocyte lipid accumulation

The consumption of HFD enhanced mice body weight in a time-dependent manner. D1 mice fed with HFD for short-term had significant gain in body weight ($P< 0.05$ *vs* C1); the difference was more pronounced ($P< 0.001$) in the moderate- and prolonged-term feeding when D2 and D3 mice were compared with their respective age-matched controls indicating gradual onset of obesity (Fig. 2a). Blood glucose level was similarly augmented in HFD groups ($P< 0.001$) with respect to control confirming hyperglycemia (Fig. 2b). We performed oral glucose tolerance test (OGTT) in control and diabetic groups, and results are shown in (Fig. 2c). With increasing duration of HFD feeding, progressive loss in the ability of glucose clearance in condition of glucose overload was observed although control mice showed proper blood glucose regulation. At the time points measured, all diabetic mice exhibited consistently higher levels of blood glucose ($P< 0.001$) relative to their control counterparts. Thus, our experimental set up of HFD regimen for three

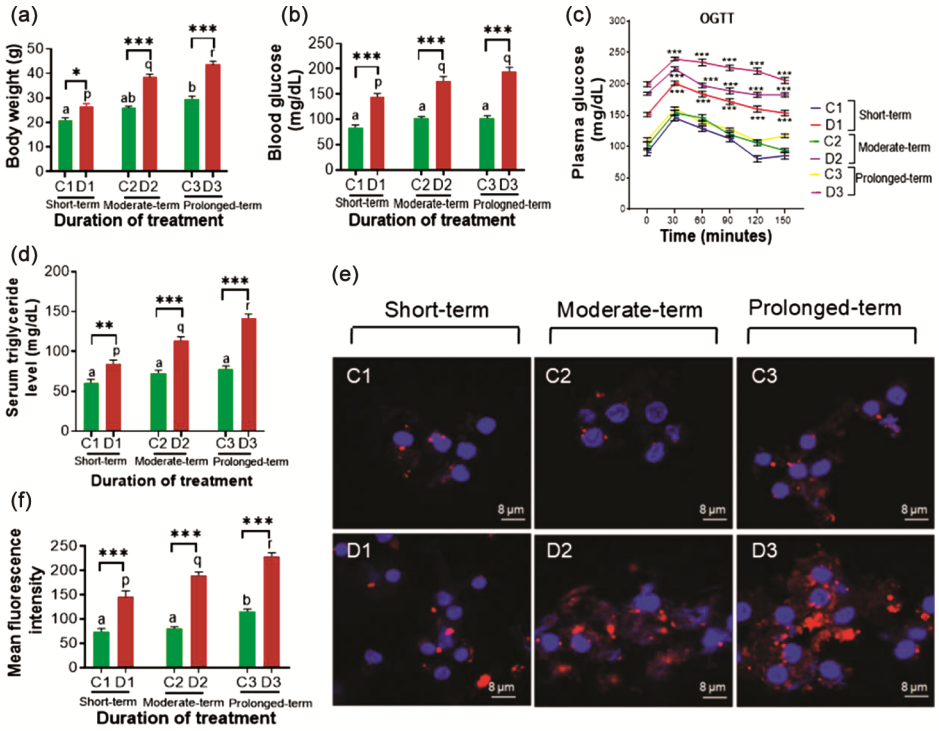

Fig. 2 — Time-dependent effects of high fat diet (HFD) upon (a) Body weight; (b) Blood glucose level; (c) Whole-body glucose tolerance by Oral Glucose Tolerance Test (OGTT); (d) Level of serum triglyceride; (e) Representative micrographs showing lipid accumulation in isolated hepatocytes stained with Oil Red O; and (f) Quantification of its fluorescence intensity. The animal groups shown here are obese diabetic mice raised by feeding HFD for different durations, short-term D1 (4-week), moderate-term D2 (16-week) and prolonged-term D3 (32-week), and their corresponding control mice (C1, C2 and C3, respectively). Data are presented as mean ± SEM (n=6). *P* value less than 0.05 was considered significant. Different letters indicate significance within groups (for control mice: a, b, and c; for obese diabetic mice: p, q, and r, respectively). Statistical significance between obese diabetic mice *vs* their age-matched control are indicated as $*P < 0.05$, $**P < 0.01$ and $***P < 0.001$

different time durations developed obese insulin-resistant hyperglycemic mice models. The consumption of lipid-enriched diet leads to obesity which is accompanied by altered glucose and lipid metabolism[19]. Similarly, we found that serum triglyceride levels were significantly elevated in HFD-fed groups in a time-dependent fashion (Fig. 2d). We checked lipid accumulation within hepatocytes with ORO staining. The micrographs are presented in (Fig. 2e) followed by quantification of fluorescent intensity shown in (Fig. 2f). The nuclei are stained blue with DAPI while lipid-capturing ORO fluorescent stain appears red. With progression of time, increased intracellular accumulation of lipid was evident in D1, D2 and D3 groups with respect to their age-matched control counterparts suggesting hepatic lipid accumulation. As HFD feeding proceeded from short-term to moderate and then to prolonged-term, we observed significant gain in body weight along with glucose intolerance, hyperglycemia and hyperlipidemia confirming onset of insulin resistance and progressive obesity-induced diabetes in the animals. This was concomitant with improper lipid metabolism such that mice hepatocytes were lipid-laden.

Time-dependent effects of HFD upon hepatocyte lipoapoptosis

In order to assess the health of hepatocytes, we performed TUNEL assay counter staining the nuclei with DAPI. The apoptotic event was noticeable in the micrographs shown in (Fig. 3a). While short-term HFD feeding did not show positive result in TUNEL assay, prominent apoptotic nuclei were seen in D2 and D3 groups compared to their age-matched controls. It is reported that glucose fluctuation and lipotoxicity can induce liver apoptosis in mice fed HFD for 8 weeks followed by glucose injection[20].We observed clear evidences of increased apoptosis in hepatocytes of mice fed with HFD for moderate-term. This is corroborated by previous report of enhanced hepatocyte apoptosis in 16-week HFD condition[21].We also calculated the percentage of TUNEL-positive cells. While C1 and C2 displayed very negligible (less

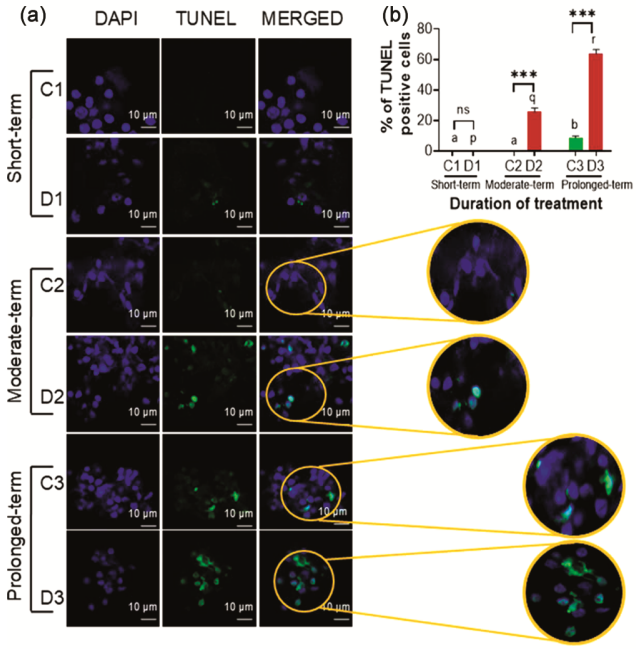

Fig. 3 — Time-dependent effects of high fat diet (HFD) upon hepatocyte lipoapoptosis as revealed by (a) Representative micrographs of TUNEL assay (middle panel) counterstained with DAPI (left panel) along with merged images (right panel); and (b) Bar diagram depicting changes in the percentage of TUNEL-positive cells. The animal groups shown here are obese diabetic mice raised by feeding HFD for different durations, short-term D1 (4-week), moderate-term D2 (16-week) and prolonged-term D3 (32-week), and their corresponding control mice (C1, C2 and C3, respectively). Data are presented as mean ± SEM (n=6). *P* value less than 0.05 was considered significant. Different letters indicate significance within groups (for control mice: a, b, and c; for obese diabetic mice: p, q, and r, respectively). Statistical significance between obese diabetic mice *vs* their age-matched control are indicated as **P* < 0.05, ***P* < 0.01 and ****P* < 0.001.

than 1%) apoptotic nuclei, the fraction of TUNEL-positive cells was very high in moderate-term HFD-fed D2 (more than 20%). C3 showed greater prevalence of apoptotic hepatocytes compared to C1 and C2 which could be ascribed as an age-dependent phenomenon. Chronic HFD feeding exacerbated liver damage as the proportion of TUNEL-positive cells was as high as 60% in D3 group (*P*< 0.001 relative to corresponding control C3). We have shown here the time-dependent effects of HFD upon hepatocyte lipoapoptosis. The severity of lipoapoptosis was almost 3-fold higher in D3 than D2 (Fig. 3b). The fraction of TUNEL-positive cells positively correlated with the escalating metabolic disturbances due to obesity and type 2 diabetes with maximum damage noticeable in the liver cells isolated from diabetic mice fed with HFD for prolonged-term.

Effect of chronic HFD upon FetA level

Obesity-induced diabetes is closely linked to FetA. Mice deficient in *Ahsg* gene had better insulin sensitivity[22]. In addition, FetA-deficient mice resisted weight gain and insulin resistance associated with aging[23]. Further research highlighted the mechanism of FetA secretion under influence of SFA, palmitate through activation of NFκB[24]. FetA released by liver in obese condition acts as an endogenous ligand for TLR4 in adipocytes; FetA actions are mediated by formation of a ternary complex comprising TLR4-FetA-SFA that could activate downstream signal transduction of TLR4 eliciting inflammatory responses[17]. This is exacerbated by FetA-induced macrophage chemotaxis and its polarization toward inflammatory subtype in adipose tissue leading to insulin resistance[25]. Short-term HFD feeding for three days resulted in heightened expression of *Ahsg* mRNA and serum FetA level[26]. These authors also demonstrated hepatocytes as the site of FetA production. In the present study, immunoblotting analyses with *anti*-FetA revealed significantly higher expression of FetA protein in hepatocyte lysates prepared from D3 mice fed with HFD for prolonged-term when compared with its corresponding C3 control (Fig. 4a & b). In order to evaluate the particular role of FetA, we designed the next set of experiments treating the mice with FetA.

Effect of FetA upon glucose homeostasis, liver histology and ROS generation *in vivo*

Several epidemiological studies have established positive correlation between high serum FetA concentration and the occurrence of insulin resistance and type 2 diabetes[27-29]. When we performed ELISA, augmented levels of circulating FetA were recorded in sera obtained from FetA-treated mice against control, confirming the treatment (Fig. 4c). FetA-injected mice were hyperglycemic with significantly enhanced blood glucose level (*P*< 0.001) *vs* untreated control (Fig. 4d). OGTT data clearly revealed impaired glucose uptake in FetA-treated animals (Fig. 4e). Histopathological alterations including loss of hepatocyte organization, presence of apoptotic bodies (marked by dotted line) and lobular inflammation (encircled) were observed in FetA-injected mice (Fig. 4f). The reactive oxygen species (ROS) can trigger apoptosis[30]. While control mice hepatocytes had basal level of intracellular ROS, it was of interest to record almost doubled ROS level in hepatocytes isolated from FetA-treated mice showing elevated oxidative stress (Fig. 4g).

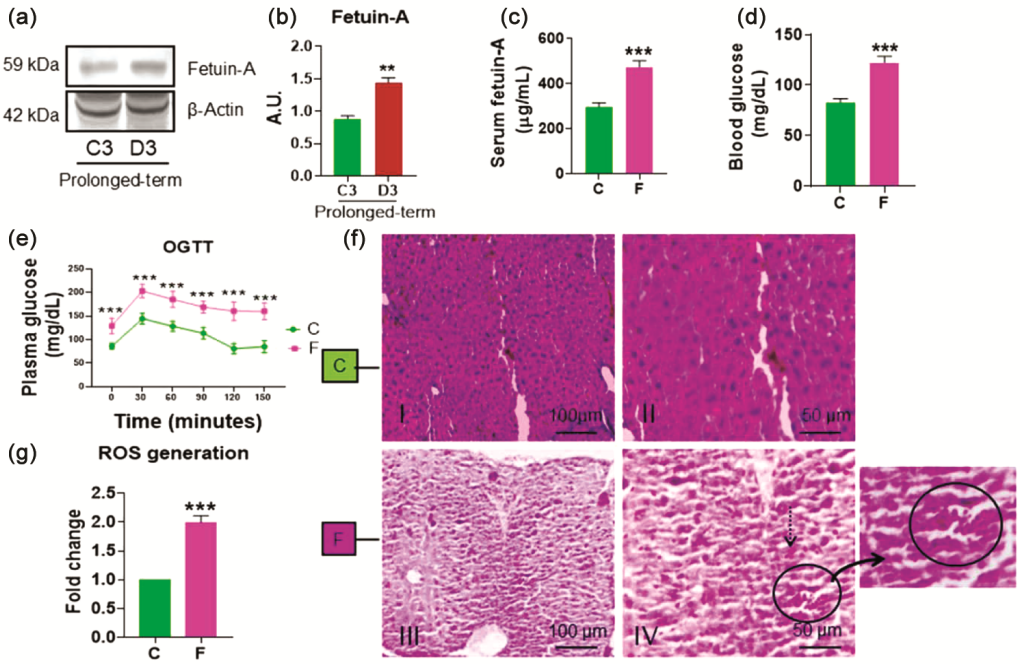

Fig. 4 — (a) Effect of chronic high fat diet (HFD) upon expression of fetuin-A (FetA) protein in hepatocyte lysates prepared from D3 mice fed with HFD for prolonged-term and corresponding C3 control as assessed by immunoblotting; and (b) its densitometric analyses; (c) Bar diagram depicting changes in the circulating levels of FetA in sera obtained from FetA-treated mice and its control as determined by ELISA; Effect of FetA upon (d) Blood glucose level; and (e) Whole-body glucose tolerance by Oral Glucose Tolerance Test (OGTT); (f) Representative micrographs showing histopathological alterations including loss of hepatocyte organization, presence of apoptotic bodies (marked by dotted line) and lobular inflammation (encircled) in FetA-injected mice; and (g) Bar diagram depicting fold change in intracellular ROS level measuring fluorescence intensity of DCFDA-stained hepatocytes isolated from FetA-treated mice over its control. Data are presented as mean ± SEM (n=6 for biochemical analyses; n=3 for immunoblotting and histology). *P* value less than 0.05 was considered significant. Statistical significance between chronic obese diabetic mice (D3) *vs* age-matched control (C3), and between FetA-injected mice (F) and its control (C) are indicated as **P* < 0.05, ***P* < 0.01 and ****P* < 0.001

Effect of FetA upon key apoptotic marker proteins *in vivo* and *in vitro*

In streptozotocin-induced diabetic rats, high oxidative stress-induced mitochondrial membrane permeability transition pore opening is reported[31]. Hyperglycemia inflicted mitochondrial damage and cell death due to release of pro-apoptotic proteins in the cytoplasm[32]. Palmitic acid promoted ER stress and apoptosis in hepatoma cells[33]. In our HFD-fed mice models, lipotoxic condition triggered apoptosis in hepatocytes as shown by TUNEL assay. With an aim to discern the specific role of FetA in apoptosis, immunoblotting of key apoptotic markers was carried out with hepatocyte lysates prepared from FetA-treated mice (Fig. 5a). The densitometric analyses showed significant downregulation of anti-apoptotic protein Bcl-2 (Fig. 5b) and upregulation of pro-apoptotic BAX (Fig. 5c). Similar rise in BAX was reported in HFD-fed rats[34]. The balance of these proteins is vital for cellular health. We found significantly higher BAX:Bcl-2 ratio ($P < 0.001$) compared to control (Fig. 5d). On a similar note, Apaf-1 (Fig. 5e) and Cyt c (Fig. 5g) upregulation was observed in FetA-administered group. Control and treated mice showed no change in total Caspase-9 protein expression in the hepatocytes (Fig. 5g). However, cleaved product of Caspase-9 was highly expressed in FetA-treated group (Fig. 5h). The ratio of total Caspase-9 to its cleaved form was notably enhanced in the treated animals than their control counterparts (Fig. 5i) indicating high FetA concentration is related to liver cell death.

We further validated this in an *in vitro* experimental set up. We isolated hepatocytes from control mice and then treated these with palmitate and FetA for confirming apoptotic markers by immunoblotting (Fig. 6a) followed by densitometry. Treatment of hepatocytes with palmitate alone was done to mimic lipid-rich microenvironment. Palmitate can directly affect mitochondrial membrane potential and induce intrinsic pathway[35]. High ROS level initiated apoptosis in palmitate-exposed hepatocytes[38]. On a similar note, we observed palmitate exposure

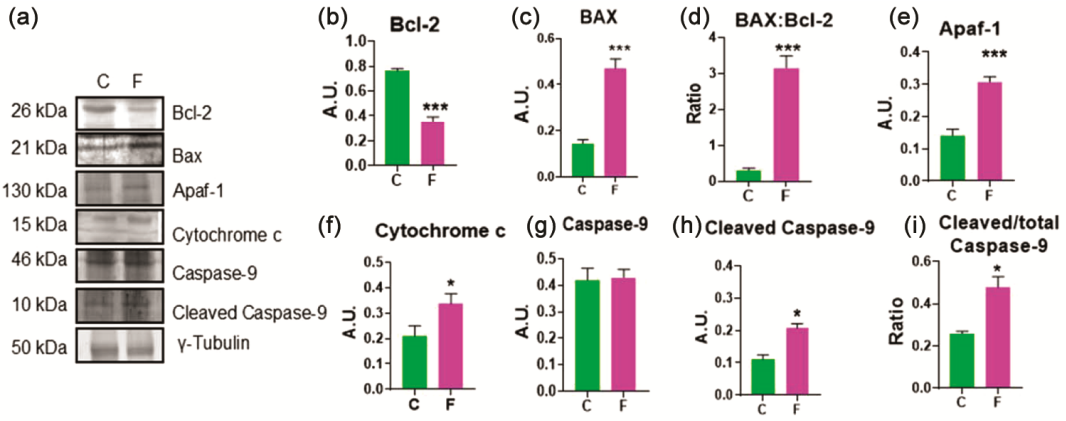

Fig. 5 — (a) Representative immunoblots showing effect of FetA upon key apoptotic marker proteins *in vivo* as revealed by immunoblotting carried out with hepatocyte lysates prepared from FetA-treated mice (F) and its control (C); and bar diagrams depicting densitometric analyses of (b) Bcl-2; (c) BAX; (d) BAX:Bcl-2 ratio; (e) Apaf-1; (f) cytochrome c; (g) total Caspase-9; (h) cleaved Caspase-9; and (i) cleaved Caspase-9:total Caspase-9 ratio. Data are presented as mean ± SEM (n=3). *P* value less than 0.05 was considered significant. Statistical significance between FetA-injected mice (f) and its control (c) are indicated as $*P < 0.05$, $**P < 0.01$ and $***P < 0.001$

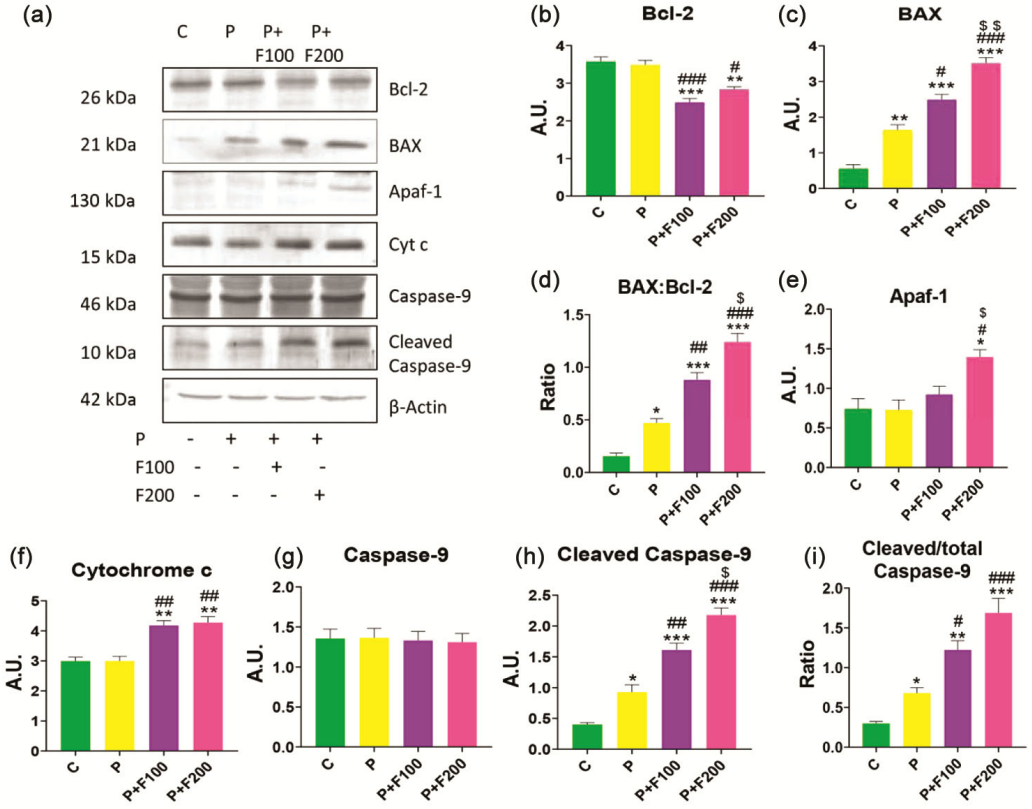

Fig. 6 — (a) Representative immunoblots showing effect of FetA upon key apoptotic marker proteins *in vitro* as revealed by immunoblotting carried out with lysates of mice hepatocytes treated without (control, C) and with 0.75 mM palmitate only (P), or palmitate conjugated-FetA at two different concentrations (100 µg/mL and 200 µg/mL); and bar diagrams depicting densitometric analyses of (b) Bcl-2; (c) BAX; (d) BAX:Bcl-2 ratio; (e) Apaf-1; (f) cytochrome c; (g) total Caspase-9; (h) cleaved Caspase-9; and (i) cleaved Caspase-9:total Caspase-9 ratio. Data are presented as mean ± SEM (n=3 independent experiments). *P* value less than 0.05 was considered significant. Statistical significance is denoted by $*P < 0.05$, $**P < 0.01$ and $***P < 0.001$ *vs* Control (C); $^{\$}P < 0.05$, $^{\$\$}P < 0.01$ and $^{\$\$\$}P < 0.001$ *vs* Palmitate conjugated-FetA at 100 µg/mL (P+F100); and $^{\#}P < 0.05$, $^{\#\#}P < 0.01$ and $^{\#\#\#}P < 0.001$ *vs* Palmitate only (P)

upregulated BAX; however, presence of FetA inhibited Bcl-2 while inducing BAX thereby increasing BAX:Bcl-2 ratio in a dose-dependent manner (Fig. 6b-d). Similar trend was seen for Apaf-1 (Fig. 6e) and Cyt c (Fig. 6f). The appearance of cleaved Caspase-9 and increasing ratio of total Caspase-9 to its cleaved form was more prominent in Fet-A exposed cells compared to only palmitate-treated cells (Fig. 6g-i), thereby providing evidences of its pro-apoptotic effect in hepatocytes.

Conclusion

FetA, at high levels, promoted metabolic impairment in mice involving insulin resistance, hyperglycemia, and failure of adequate glucose uptake from blood. The presence of FetA disturbed pro-apoptotic:anti-apoptotic protein balance in the hepatocytes in favour of the former resulting in histopathological alterations in liver as evident from apoptotic bodies, hepatocyte disorganization and lobular inflammation, and high oxidative stress, indicators of liver injury and death. In lipid-laden hepatocytes, FetA was a potential inducer of mitochondrial cell death. Taken together, our *in vivo* and *in vitro* experiments put forth the pivotal role of FetA-mediated hepatocyte lipoapoptosis in exacerbating liver damage associated with obesity and type 2 diabetes.

Acknowledgement

The authors gratefully acknowledge the Head, Department of Zoology (supported by UGC-CAS and DST-FIST, Govt. of India), Visva-Bharati, Santiniketan for providing infrastructural facilities. Suktara Guria thanks CSIR, Govt. of India for junior and senior research fellowships.

Conflict of interest

Both the authors declare no conflict of interest.

References

1 Lin X & Li H, Obesity: epidemiology, pathophysiology, and therapeutics. *Front Endocrinol*, 12 (2021) 706978.

2 Snel M, Jonker JT, Schoones J, Lamb H, de Roos A, Pijl H, Smit JW, Meinders AE & Jazet IM, Ectopic fat and insulin resistance: pathophysiology and effect of diet and lifestyle interventions. *Int J Endocrinol*, 2012 (2012) 983814.

3 Goedeke L, Strober JW, Suh R, Paolella LM, Li X, Rogers JC, Petersen MC, Nasiri AR, Casals G, Kahn M & Cline GW, High-fat-diet-induced hepatic insulin resistance per se attenuates murine de novo lipogenesis. *iScience*, 27 (2024) 111175.

4 Sanders FW & Griffin JL, De novo lipogenesis in the liver in health and disease: more than just a shunting yard for glucose. *Biol Rev Cam Philos Soc*, 91 (2016) 452.

5 Ferreira DM, Castro RE, Machado MV, Evangelista T, Silvestre A, Costa A, Coutinho J, Carepa F, Cortez-Pinto H & Rodrigues CM, Apoptosis and insulin resistance in liver and peripheral tissues of morbidly obese patients is associated with different stages of non-alcoholic fatty liver disease. *Diabetologia*, 54 (2011) 1788.

6 Civera M, Urios A, Garcia-Torres ML, Ortega J, Martinez-Valls J, Cassinello N, Del Olmo JA, Ferrandez A, Rodrigo JM & Montoliu C, Relationship between insulin resistance, inflammation and liver cell apoptosis in patients with severe obesity. *Diabetes Metab Res Rev*, 26 (2010) 187.

7 Cusi K, Chang Z, Harrison S, Lomonaco R, Bril F, Orsak B, Ortiz-Lopez C, Hecht J, Feldstein AE, Webb A, Louden C, Goros M & Tio F, Limited value of plasma cytokeratin-18 as a biomarker for NASH and fibrosis in patients with non-alcoholic fatty liver disease. *J Hepatol*, 60 (2014) 167.

8 Mandelia C, Collyer E, Mansoor S, Lopez R, Lappe S, Nobili V & Alkhouri N, Plasma cytokeratin-18 level as a novel biomarker for liver fibrosis in children with nonalcoholic fatty liver disease. *J Pediatr Gastroenterol Nutr*, 63 (2016) 181.

9 Unger RH, Lipotoxic diseases. *Annu Rev Med,* 53 (2002) 319.

10 Malhi H & Gores GJ, Molecular mechanisms of lipotoxicity in nonalcoholic fatty liver disease. *Semin Liver Dis*, 28 (2008) 360.

11 Jung TW, Yoo HJ & Choi KM, Implication of hepatokines in metabolic disorders and cardiovascular diseases. *BBA Clin*, 5 (2016) 108.

12 Lin X, Braymer HD, Bray GA & York DA, Differential expression of insulin receptor tyrosine kinase inhibitor (fetuin) gene in a model of diet-induced obesity. *Life Sci*, 63 (1998) 145.

13 Stefan N, Hennige AM, Staiger H, Machann J, Schick F, Kröber SM, Machicao F, Fritsche A & Häring HU, α2-Heremans-Schmid glycoprotein/fetuin-A is associated with insulin resistance and fat accumulation in the liver in humans. *Diabetes Care*, 29 (2006) 853.

14 Bourebaba L & Marycz K, Pathophysiological implication of fetuin-A glycoprotein in the development of metabolic disorders: a concise review. *J Clin Med*, 8 (2019) 2033.

15 Ghosh S & Mukherjee S, Testicular germ cell apoptosis and sperm defects in mice upon long-term high fat diet feeding. *J Cell Physiol*, 233 (2018) 6896.

16 Chattopadhyay D, Das S, Guria S, Basu S & Mukherjee S, Fetuin-A regulates adipose tissue macrophage content and activation in insulin resistant mice through MCP-1 and iNOS: involvement of IFNγ-JAK2-STAT1 pathway. *Biochem J*, 478 (2021) 4027.

17 Pal D, Dasgupta S, Kundu R, Maitra S, Das G, Mukhopadhyay S, Ray S, Majumdar SS & Bhattacharya S, Fetuin-A acts as an endogenous ligand of TLR4 to promote lipid-induced insulin resistance. *Nat Med*, 18 (2012) 1279.

18 Lowry OH, Rosebrough NJ, Farr AL & Randall RJ, Protein measurement with the Folin phenol reagent. *J Biol Chem*, 193 (1951) 265.

19 Lackey DE, Lazaro RG, Li P, Johnson A, Hernandez-Carretero A, Weber N, Vorobyova I, Tsukomoto H & Osborn O, The role of dietary fat in obesity-induced insulin resistance. *Am J Physiol Endocrinol Metab*, 311 (2016) E989.

20 Yin X, Zheng F, Pan Q, Zhang S, Yu D, Xu Z & Li H, Glucose fluctuation increased hepatocyte apoptosis under lipotoxicity and the involvement of mitochondrial permeability transition opening. *J Mol Endocrinol*, 55 (2015) 169.
21 Soltis AR, Kennedy NJ, Xin X, Zhou F, Ficarro SB, Yap YS, Matthews BJ, Lauffenburger DA, White FM, Marto JA, Davis RJ & Fraenkel E, Hepatic dysfunction caused by consumption of a high-fat diet. *Cell Rep*, 21 (2017) 3317.
22 Mathews ST, Singh GP, Ranalletta M, Cintron VJ, Qiang X, Goustin AS, Jen KL, Charron MJ, Jahnen-Dechent W & Grunberger G, Improved insulin sensitivity and resistance to weight gain in mice null for the Ahsg gene. *Diabetes*, 51 (2002) 2450.
23 Mathews ST, Rakhade S, Zhou X, Parker GC, Coscina DV & Grunberger G, Fetuin-null mice are protected against obesity and insulin resistance associated with aging. *Biochem Biophys Res Commun*, 350 (2006) 437.
24 Dasgupta S, Bhattacharya S, Biswas A, Majumdar SS, Mukhopadhyay S, Ray S & Bhattacharya S, NF-κB mediates lipid-induced fetuin-A expression in hepatocytes that impairs adipocyte function effecting insulin resistance. *Biochem J*, 429 (2010) 451.
25 Chatterjee P, Seal S, Mukherjee S, Kundu R, Mukherjee S, Ray S, Mukhopadhyay S, Majumdar SS & Bhattacharya S, Adipocyte fetuin-A contributes to macrophage migration into adipose tissue and polarization of macrophages. *J Biol Chem*, 288 (2013) 28324.
26 Lanthier N, Lebrun V, Molendi-Coste O, van Rooijen N & Leclercq IA, Liver fetuin-A at initiation of insulin resistance. *Metabolites*, 12 (2022) 1023.
27 Ix JH, Shlipak MG, Brandenburg VM, Ali S, Ketteler M & Whooley MA, Association between human fetuin-A and the metabolic syndrome: data from the Heart and Soul Study. *Circulation*, 113 (2006) 1760.
28 Jung CH, Kim BY, Kim CH, Kang SK, Jung SH & Mok JO, Associations of serum fetuin-A levels with insulin resistance and vascular complications in patients with type 2 diabetes. *Diab Vasc Dis Res*, 10 (2013) 459.
29 Aroner SA, St-Jules DE, Mukamal KJ, Katz R, Shlipak MG, Criqui MH, Kestenbaum B, Siscovick DS, de Boer IH, Jenny NS, Budoff MJ, Ix JH & Jensen MK, Fetuin-A, glycemic status, and risk of cardiovascular disease: the multi-ethnic study of atherosclerosis. *Atherosclerosis*, 248 (2016) 224.
30 Kannan K & Jain SK, Oxidative stress and apoptosis. *Pathophysiology*, 7 (2000) 153.
31 Daniel OO, Adeoye AO, Ojowu J & Olorunsogo OO, Inhibition of liver mitochondrial membrane permeability transition pore opening by quercetin and vitamin E in streptozotocin-induced diabetic rats. *Biochem Biophys Res Commun*, 504 (2018) 460.
32 Dey A & Swaminathan K, Hyperglycemia-induced mitochondrial alterations in liver. *Life Sci*, 87 (2010) 197.
33 Zhang Y, Xue R, Zhang Z, Yang X & Shi H, Palmitic and linoleic acids induce ER stress and apoptosis in hepatoma cells. *Lipids Health Dis*, 11 (2012) 1.
34 Wang Y, Ausman LM, Russell RM, Greenberg AS & Wang XD, Increased apoptosis in high-fat diet–induced nonalcoholic steatohepatitis in rats is associated with c-Jun NH2-terminal kinase activation and elevated proapoptotic Bax. *J Nutr*, 138 (2008) 1866.
35 de Pablo MA, Susin SA, Jacotot E, Larochette N, Costantini P, Ravagnan L, Zamzami N & Kroemer G, Palmitate induces apoptosis *via* a direct effect on mitochondria. *Apoptosis*, 4 (1999) 81.